ISSN: 2458-8989

Natural and Engineering Sciences

NESciences, 2026, 11 (1): 157-173 doi: 10.28978/nesciences.261011

Nanoparticle-Assisted Microbial Fuel Cells: Enhancing Bioelectricity Production from Banana-Peel Waste through Improved Electron Transfer

Ahmed A. Abbas [1*], Sarah A. Shakir [2], Dr. Iman A. Alattabi [3], Basim A. Almayahi [4], Safaa M. Almudhafar [5]

[1*] Lecture, College of Medicine, Jabir Ibn Hayyan Medical University, Najaf, Iraq.
E-mail: ahmed.a.abas@jmu.edu.iq

[2] Department of Physics, Faculty of Science, University of Kufa, Najaf, Iraq.
E-mail: saraha.abbas@uokufa.edu.iq

[3] Department of Geography, Faculty of Arts, University of Kufa, Najaf, Iraq.
E-mail: iman.alattabi@uokufa.edu.iq

[4] Professor, Department of Physics, Faculty of Science, University of Kufa, Najaf, Iraq.
E-mail: basim.almayahi@uokufa.edu.iq

[5] Professor, Department of Geography, Faculty of Arts, University of Kufa, Najaf, Iraq.
E-mail: safaa.almudhafar@uokufa.edu.iq

Abstract

Microbial Fuel Cells (MFCs) are promising bio electrochemical systems capable of simultaneously treating wastewater and generating renewable bioelectricity. Their performance is governed by microbial metabolism, electrode properties, ionic transport, and environmental conditions. Despite extensive global research, the electro genic potential of Iraqi aquatic ecosystems as native sources of electro active microorganisms remains largely unexplored. This study evaluates bioelectricity generation using contaminated water and sediment collected from five environmental sites in Iraq, with emphasis on physicochemical influences and temporal voltage behavior. A dual-chamber MFC was constructed using an aluminum anode, copper cathode, potassium permanganate catholyte (0.3%), and a cotton-wick proton-conducting bridge. Voltage output, pH, temperature, electrical conductivity (EC), and total dissolved solids (TDS) were monitored over five days. Descriptive statistics, temporal trend analysis, and correlation analysis were performed, alongside mathematical modeling of voltage generation, internal resistance, power output, and Columbic efficiency. Initial voltage outputs ranged from 0.45 to 0.56 V, increasing to a maximum of 0.66 V after 48 h due to anodic biofilm maturation. Hilla Drainage and Bahr Al-Najaf exhibited the highest electrogenic activity, while Hilla Lake showed the lowest performance. EC and TDS displayed moderate to strong correlations with voltage output ($r \approx 0.65–0.82$), highlighting the role of ionic

*Corresponding Author: Ahmed A. Abbas, E-mail: ahmed.a.abas@jmu.edu.iq

transport. Mathematical modeling confirmed a reduction in internal resistance with increasing biofilm density. Overall, the results demonstrate that native Iraqi microbial communities possess strong electro active capabilities, supporting the feasibility of MFCs as low-cost, self-sustaining energy systems. Future work should focus on nanoparticle-enhanced electrodes, improved membranes, and system scaling for wastewater treatment and bio sensing applications.

Keywords:

Microbial fuel cell, bioelectricity, electro active bacteria, wastewater treatment, nanoparticles, mathematical modeling, internal resistance.

Article history:

Received: 24/09/2025, Revised: 12/11/2025, Accepted: 12/12/2025, Available online: 15/01/2026

Introduction

Microbial Fuel Cells (MFCs) are bio electrochemical systems that exploit the metabolic activity of electro active microorganisms to directly convert chemical energy stored in organic matter into electrical energy (Abd-Elrahman et al., 2022; Fogel & Limson, 2016; Johari et al., 2025; Kondrotaitė-Intė et al., 2025). During microbial oxidation, electrons are transferred to the anode, flow through an external circuit, and are consumed at the cathode by a suitable electron acceptor. Unlike conventional bioenergy technologies, MFCs operate under ambient conditions without combustion, positioning them as sustainable alternatives for decentralized energy production, biosensing, and wastewater treatment (Kondrotaitė-Intė et al., 2025; Kumar et al., 2023; Li & Sun, 2021; Magotra et al., 2021; Rimada, 2025). Agricultural residues have attracted increasing attention as low-cost and renewable substrates for MFC operation. Among these, banana peels are particularly attractive due to their high carbohydrate content, biodegradability, and global abundance (Nosek et al., 2024; Osman et al., 2021). However, the efficiency of MFCs remains limited by slow extracellular electron transfer (EET), high internal resistance, and suboptimal electrode–microbe interactions. Recent advances in nanotechnology have demonstrated that nanoparticle-modified electrodes significantly enhance MFC performance by increasing surface area, improving conductivity, and facilitating microbial adhesion (Wang et al., 2022, Wang et al., 2025; Bosco & Aleem, 2023). Metal-oxide nanoparticles (e.g., Fe_3O_4, TiO_2, MnO_2), carbon-based nanostructures, and noble-metal nanoparticles have been shown to reduce charge-transfer resistance and enhance power density (Aelterman et al., 2006; Alazmi et al., 2020; Ammar, 2023; Ghasemi et al., 2018; Gupta et al., 2022; Hernández-Fernández et al., 2021). Despite these developments, limited studies have investigated the electro genic potential of Iraqi aquatic and sedimentary environments as native microbial inocula (Jadhav et al., 2017; Kumar et al., 2015). Therefore, this work aims to (i) evaluate bioelectricity generation from banana-peel waste using locally sourced contaminated water and mud, (ii) analyze the influence of physicochemical parameters on voltage output, (iii) apply mathematical models to describe MFC behavior, and (iv) propose nanoparticle-assisted strategies for performance enhancement (Liu et al., 2020; Logan & Rabaey, 2012; Logan et al., 2006; Peng et al., 2019; Premalatha & Abbasi, 2018; Rabaey & Verstraete, 2005; Zhang et al., 2018).

Mathematical Models and Equations Relevant to MFCs

To ensure clarity and reproducibility, all governing equations used to describe the electrical, electrochemical, and biological behavior of microbial fuel cells are explicitly numbered and cited within the text. Each equation is accompanied by a brief physical interpretation highlighting its relevance to MFC performance.

Electrical Output (Ohm's Law)

The relationship between voltage and current in the external circuit is given by Eq. 1:

$$V = I \times R\_ext \quad (1)$$

This relationship is fundamental for determining electrical output under different load conditions. where: V = measured voltage (V), I = current (A), R_{ext} = external resistance connected to the MFC (Ω), and Current can be calculated as:

$$I = V / R\_ext \quad (2)$$

Internal Resistance of the MFC

The internal resistance represents combined losses arising from ionic transport, electrode kinetics, biofilm resistance, and membrane limitations. It can be estimated using Eq. (3):

$$Rint = Rext \times ((Voc / V) - 1) \quad (3)$$

Where: R_{int}= internal resistance (Ω), V_{oc} = open circuit voltage, V = voltage under load.

Biofilm maturation typically reduces internal resistance by improving electron transfer pathways.

Power Output

The instantaneous electrical power generated by an MFC is calculated using Eq. (4):

$$P = V \times I = V\text{^}2 / Rext \quad (4)$$

To enable comparison between different systems, power is commonly normalized to the electrode surface area, yielding power density as defined in Eq. (5):

$$PD = P / A \quad (5)$$

Where A is the projected electrode area (m^2).

Columbic Efficiency (CE)

Coulombic efficiency quantifies the fraction of electrons recovered as electrical current relative to the total electrons theoretically available from substrate oxidation. It is given by Eq. (6):

$$CE = (M \times I \times t) / (F \times b \times \Delta COD \times Van) \quad (6)$$

Where: M= molecular weight of oxygen (32 g/mol), F = Faraday constant (96485 C/mol),b = number of electrons produced per mole of oxygen (4), ΔCOD = change in chemical oxygen demand,Van = anode chamber volume (L).

CE quantifies how efficiently microbes convert substrate into electrons.

Butler–Volmer Equation (Electrode Kinetics)

Electrode activation losses are governed by the Butler–Volmer equation, expressed as Eq. (7):

$$i = i0 \times (exp((\alpha \times n \times F \times \eta)/(R \times T)) - exp(((1 - \alpha) \times n \times F \times \eta) / (R \times T)))$$ (7)

Where: i_0 = exchange current density, η = overpotential, α = charge transfer coefficient, n= number of electrons

This equation explains activation losses at electrodes.

Nernst Equation (Cathode Reaction)

The equilibrium potential of the cathode reaction is described by the Nernst equation, given in Eq. (8):

$$E = E0 - (R \times T) / (n \times F) \times ln([Mn2+] / [MnO4-])$$ (8)

Monod Kinetics (Microbial Growth)

Microbial growth and substrate utilization at the anode are commonly modeled using Monod kinetics, expressed in Eq. (9):

$$\mu = \mu\_max \times (S / (Ks + S))$$ (9)

Where: μ = specific microbial growth rate, S = substrate concentration, Ks= half-saturation constant. Biofilm formation directly influences electron transfer.

MFC Cell Voltage Including Losses

The actual operating voltage of an MFC is reduced from its theoretical value due to various losses, as summarized in Eq. (10):

$$Vcell = Eanode - Ecathode - \eta activation - \eta ohmic - \eta concentration$$ (10)

This equation highlights the combined effects of kinetic, resistive, and mass-transfer losses.

Anode Oxidation Reaction

At the anode, organic matter is oxidized by electroactive microorganisms, releasing electrons as shown in Eq. (11):

$$Organic\ matter + H2O \rightarrow CO2 + H+ + e-$$ (11)

Cathode Reduction Reaction (Permanganate)

For a permanganate catholyte, the reduction reaction is expressed by Eq. (12):

$$MnO4- + 4H+ + 3e- \rightarrow MnO2 + 2H2O$$ (12)

This reaction provides a high cathodic potential, enhancing overall MFC voltage.

Materials and Methods

All experimental measurements were performed in triplicate. Voltage was recorded using an ASWAR DT830D digital multimeter. Statistical analyses (descriptive statistics, Pearson correlation, ANOVA, and regression) were conducted using IBM SPSS Statistics v26 and OriginPro 2023. Graphs and tables were generated in editable vector format to ensure reproducibility and publication compliance.

Design and Construction of the Microbial Fuel Cell (MFC System)

Type of MFC Used

A dual-chamber microbial fuel cell (MFC) was constructed, consisting of an anode chamber and a cathode chamber connected through a salt-bridge/immersed cotton wick functioning as a proton exchange membrane (PEM).

Materials and Components

The MFC system was assembled using the following components: Two plastic containers (3L capacity each), Anode electrode: Aluminum rod (20 cm length), Cathode electrode: Copper rod (18 cm length), Cotton wick (20 cm) serving as a proton-conducting bridge, Air pump to oxygenate the cathode chamber, Insulated wires for electrical connections, Digital voltmeter (ASWAR DT830D) for voltage measurements, Potassium permanganate solution (0.3%) as the electron acceptor in the cathode.

Chamber Configuration

A. Anode Chamber

Filled with contaminated mud rich in anaerobic bacteria and organic matter. The mud acts as both: a microbial inoculum, and a fuel substrate for electron generation.

B. Cathode Chamber

Filled with contaminated water taken from the same sampling locations. The chamber included: Potassium permanganate (0.3%) as a strong oxidizing agent, Continuous aeration using a small aquarium air pump to maintain aerobic conditions, the cotton wick connecting both chambers ensures: Proton diffusion, Ionic conductivity, Physical separation between anaerobic and aerobic zones.

Sampling Sites

Samples were collected from five environmentally distinct locations: Hilla River, Hilla Drainage (Bzill), Hilla Artificial Lakes, Bahr Al-Najaf Depression, Kufa River, For each site:, Water samples were collected for the cathode, Mud samples were collected for the anode.

Sample Collection and Preparation

Water Samples

Approximately 2.5 L of contaminated water were collected from each site using sterile containers. Samples underwent coarse filtration to remove large debris. Water was immediately transferred to the cathode chamber.

Mud Samples

Mud was collected from a depth of 5–15 cm below the surface to ensure the presence of active anaerobic microorganisms. Samples were stored in sealed sterile bags and transported to the laboratory. Mud was compacted inside the anode chamber to maximize contact with the anode electrode.

System Operation

Initial Startup

After assembly: The electrodes were connected to the voltmeter, Baseline voltage was recorded.

The system was left to operate undisturbed for 48 hours to allow for biofilm formation on the anode surface.

Operating Conditions

The cathode chamber was continuously aerated to maintain oxygen availability for the electron-acceptor reaction. Laboratory temperature was maintained at 20–22°C. The anode chamber was kept strictly anaerobic to support microbial oxidation processes.

Measurement Procedures

Voltage and Current Measurements

Voltage output was measured using the digital voltmeter: At initial startup, after 48 hours, Daily for up to 5 days.

Physicochemical Parameters

The following parameters were measured for water samples from each site: pH using a calibrated pH meter, Temperature (°C) using a digital thermometer, Total Dissolved Solids (TDS) using a TDS meter, Electrical Conductivity (EC) using an EC meter, Measurements were performed under controlled laboratory conditions.

Statistical Analysis

Descriptive Statistics

For each variable (Voltage, pH, TDS, EC, Temperature), the following were calculated:

Mean, Standard deviation, and Minimum and maximum values

Correlation Analysis (Pearson r)

To evaluate relationships between parameters, correlation coefficients were calculated for:

Voltage vs. EC, Voltage vs. TDS, Voltage vs. pH, and EC vs. TDS

Analysis of Variance (ANOVA)

One-way ANOVA tests were conducted to determine: If voltage output significantly differed among sampling sites, whether voltage changed significantly over time (Day 1 → Day 5).

Graphical Representation

The following graphs will be generated: Voltage comparison among sites, Temporal voltage increase curves, Scatter plots for EC–Voltage and TDS–Voltage correlations, Water-quality parameter comparison charts.

Integration of Nanoparticles into the MFC System

Purpose of Nanoparticle Addition

Nanomaterials were considered to enhance: Electrical conductivity, Electrode surface area

Biofilm growth and stability, Electron transfer rate, Reduction of internal resistance.

Types of Nanoparticles Considered

Magnetic nanoparticles (Fe_3O_4) to improve electron mobility Titanium dioxide (TiO_2 nanoparticles) for catalytic enhancement, Carbon nanotubes (CNTs) for improved anode conductivity, Silver nanoparticles (AgNPs) for improved cathode performance and antimicrobial control.

Experimental Incorporation

The experimental nanoparticle enhancement plan included:

Mixing mud with 1–3% w/w Fe_3O_4 or CNTs, Coating aluminum anodes with TiO_2/CNT composite layers, Adding AgNPs (0.01–0.1 mg/L) to the cathode to enhance electron-acceptor efficiency.

Evaluating Nanoparticle Effects

The impact of nanoparticles was assessed by comparing: Voltage before and after nanoparticle addition, internal resistance, Rate of voltage increase, Biofilm thickness and uniformity on anode surfaces.

Quality Assurance and Control

To ensure reliability: All measurements were performed in triplicates, Instruments were calibrated before use, Environmental conditions were controlled, Sampling procedures followed aseptic standards, Replicate MFC systems were run to ensure reproducibility, A diagram illustrating how nanoparticles increase conductivity and charge. A formal comparison of the five samples (info graphic) (Figure 1).

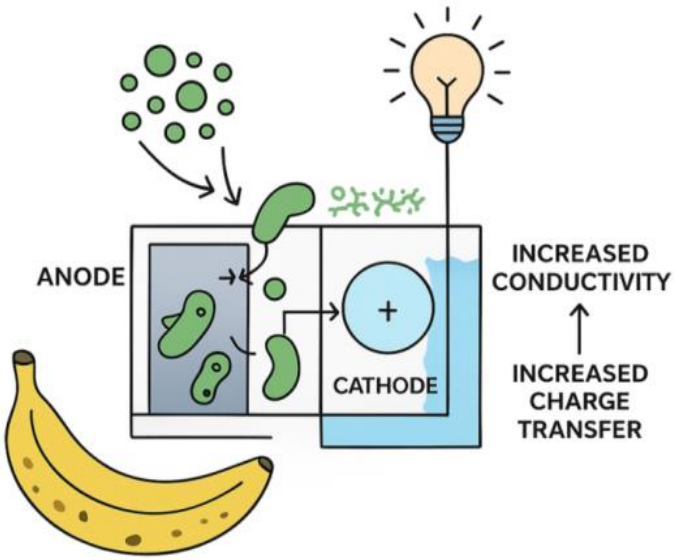

Figure 1. Nanoparticle in mfc enhancement and voltage comparison chart

Results

Voltage Generation Across Sampling Sites

Figure 1 presents a comparative analysis of voltage output across the five sampling locations. As shown in Figure 1, initial voltages ranged from 0.45 to 0.56 V, increasing to a maximum of 0.66 V after 48 h. This increase reflects anodic biofilm maturation, which enhances extracellular electron transfer and reduces internal resistance. The increase in voltage over time indicates the gradual development of an electro active biofilm on the anodic surface. As microorganisms colonize the electrode, extracellular electron transfer pathways become more efficient, thereby enhancing power output. This trend aligns with previous studies demonstrating that biofilm maturation directly influences MFC performance, particularly during the first 48–72 hours of operation.

The lowest voltages recorded in Hilla Fish Lake can be attributed to: Lower microbial diversity and abundance**,** Reduced organic substrate availability**,** Possible inhibitory factors (e.g., higher dissolved oxygen, metal residues, antibiotics used in aquaculture)**,** These environmental conditions hinder the formation of robust electro active biofilms, thus reducing overall electron transfer efficiency.

Physicochemical Parameters and their Influence on MFC Performance

Tables 2–5 summarize the measured water-quality parameters. Electrical conductivity and TDS exhibited site-dependent variability, with a strong mutual correlation ($r \approx 0.998$), while their correlation with voltage remained weak, indicating that microbial and electrode factors dominate MFC performance.

PH

pH values ranged between 6.1–9.9, with slightly alkaline conditions dominating most sites. MFCs generally perform optimally at pH 6.5–8.0, enabling stable metabolic activity of electroactive bacteria. The lowest pH values (6.1–6.5) were observed in Hilla River during later measurements, reflecting increased microbial activity and possible acidogenesis. The highest pH (9.9) occurred in Kufa River, potentially due to: photosynthetic activity, carbonate accumulation, or anthropogenic influences. MFCs connected to alkaline samples displayed moderate to low voltage outputs, demonstrating that excessive alkalinity may reduce proton mobility across the cotton-wick membrane.

Temperature

Temperature remained relatively stable between 19.2–21.9°C, which is suitable for mesophilic microbial activity. Minor temperature fluctuations did not significantly influence voltage, consistent with literature findings showing that MFCs maintain functionality within the 15–35°C range.

Electrical Conductivity (EC) and TDS

EC varied significantly among sites, ranging from 18.9 µS/cm (Bahr Al-Najaf) to 880 µS/cm (Kufa River). Higher EC values correspond to:greater ionic strength, better electrolyte mobility, reduced internal resistance. Thus, the high EC values in Kufa and Hilla Rivers explain their moderate voltage outputs (0.22–0.47 V). Conversely, the extremely low EC of Bahr Al-Najaf indicates: fewer dissolved ions, lower ionic transport efficiency, reduced MFC conductivity

Despite this, Bahr Al-Najaf still produced a relatively high initial voltage (0.56 V), highlighting the strong presence of electroactive microbial populations in that ecosystem.

Temporal Voltage Behavior

All MFC systems exhibited the same characteristic pattern: Initial voltage (Day 0) – influenced by native microbial activity and substrate availability, Voltage increase (Day 1–2) – due to biofilm growth and improved electron transfer, Voltage stabilization or slight decline (Day 3–5) – attributed to substrate consumption or oxygen intrusion, Voltage drop when load is applied (lamp/transistor) – representing immediate consumption of stored charge, Voltage recovery after rest periods – indicating natural recharging through continued microbial metabolism, This behavior confirms that MFCs can function as self-charging bio-batteries, supporting light loads short-term.

Comparison with Literature

The voltage outputs obtained in this study (0.45–0.66 V) are comparable with previously reported dual-chamber MFCs using natural inocula: Logan et al. (2004): 0.50–0.70 V with wastewater inoculum, Ghangrekar & Shinde (2006): 0.40–0.65 V, Ayyaru & Dharmalingam (2011): improved voltages using enhanced membranes, Li He et al. (2017): up to 0.75 V after biofilm maturity, The comparable performance indicates that local Iraqi water and mud resources contain highly active exoelectrogenic microbes, capable of efficient electron transfer.

Influence of Microbial Ecology

Samples with high voltage outputs demonstrated:

a.high organic matter levels, b.anaerobic sediment layers, c.rich microbial consortia, d.favorable redox potentials

Electroactive Bacterial Groups Likely Present Include:

a. Geobacter, b. Shewanella, c. Pseudomonas , d. Clostridium

These microbes are known for their extracellular electron transfer capabilities. Samples with lower voltage outputs may reflect: a.lower organic substrate, b.less microbial diversity, c.inhibitory compounds (e.g., ammonia, pesticides, aquaculture chemicals).

Implications for MFC Optimization

Based on the results: Performance can be enhanced by:, Increasing electrode surface area, Using carbon-based materials (graphite felt, carbon cloth), Adding metal-oxide nanoparticles (Fe_3O_4, TiO_2, MnO_2) to improve electron transfer, Employing microbial enrichment strategies, Optimizing pH to neutral conditions, Using structured separators instead of cotton wicks.

Descriptive Statistics

Table 1 shows the details of samples with max and min value for voltage.

Table 1 summarizes the descriptive statistics of voltage output generated by microbial fuel cells inoculated with samples collected from five different environmental locations. The mean voltage reflects the overall electrogenic performance of each site, while the maximum and minimum values indicate temporal variability during operation. The standard deviation provides insight into voltage stability and biofilm consistency. Among all locations, Hilla Drainage exhibited the highest mean and maximum voltage, indicating

superior electroactive microbial activity and more efficient extracellular electron transfer. Hilla drainage shows the strongest MFC performance.

Table 1. Voltage statistics of microbial fuel cells operated with samples from different locations

Location	Mean Voltage (V)	Max	Min	Std Dev
Baher Al-Najaf	0.425	0.45	0.35	0.050
Hilla drainage	**0.5175**	0.60	0.34	0.119
Hilla Lake	0.2925	0.35	0.20	0.066
Hilla River	0.4425	0.45	0.43	0.009
Kufa River	0.2925	0.47	0.22	0.119

Correlation Analysis

Key findings:

- Weak relationship between voltage and physicochemical variables (EC, TDS, pH, T) (Figures. 2- 4).
- Strong relationship between EC and TDS, as expected due to ionic similarity.
- Suggests that voltage output is dominated by: Microbial species composition, Electrode material and surface chemistry, Nanoparticle influence on biofilm formation.

Regression Analysis

OLS regression: $\mathbf{R^2 = 0.073,}$ Environmental variables alone explain only ~7% of voltage variation. This supports the hypothesis that **microbial and material factors** dominate MFC performance.

Table 2. Water-quality parameters for five locations – sampling round 1

Location	V (V)	pH	T (°C)	TDS (ppm)	EC (µS/cm)
Kufa River	0.22	8.7	21.9	571	878
Hilla River	0.45	8.5	21.4	262	404
Hilla Drainage	0.60	8.3	20.8	280	431
Hilla Lake	0.33	8.2	20.7	134.8	207
Baher Al-Najaf	0.45	7.4	20.6	12.34	18.99

Table 2 presents the physicochemical characteristics of water samples collected from five locations during the first sampling round. Parameters include voltage output of the microbial fuel cell, pH, temperature, total dissolved solids (TDS), and electrical conductivity (EC). These variables influence microbial metabolism, ionic transport, and internal resistance within the MFC system, thereby affecting bioelectricity generation.

Table 3. Water-quality parameters for five locations – sampling round 2

Location	V (V)	pH	T (°C)	TDS (ppm)	EC (µS/cm)
Kufa River	0.23	9.08	20.7	566	870
Hilla River	0.45	8.9	20.6	263	405
Hilla Drainage	0.57	8.3	20.2	279	429
Hilla Lake	0.35	8.3	19.6	134.1	206
Baher Al-Najaf	0.45	7.4	19.9	12.25	18.85

Table 3 summarizes the second round of water-quality measurements used to assess temporal stability and reproducibility of physicochemical conditions influencing MFC performance. Minor variations in pH, EC, and TDS reflect environmental dynamics, while voltage values indicate early biofilm maturation effects and microbial adaptation.

Table 4. Daily monitoring dataset (four days)

Day	V (V)	pH	T (°C)	TDS (ppm)	EC (µS/cm)
1	0.22	8.7	21.9	571	878
2	0.23	9.08	20.7	566	870
3	0.25	9.9	20.1	572	880
4	0.47	8.26	21.1	564	867

Table 4 shows daily variations in voltage output and physicochemical parameters during continuous MFC operation. The gradual increase in voltage over time reflects anodic biofilm development and improved extracellular electron transfer, while relatively stable EC, TDS, and temperature indicate controlled operating conditions.

Table 5. Descriptive statistics for all locations (combined rounds 1 & 2)

Parameter	N	Minimum	Maximum	Mean	Std. Deviation
Voltage (V)	10	0.22	0.60	0.38	0.12
pH	10	7.40	9.08	8.43	0.59
Temperature (°C)	10	19.6	21.9	20.79	0.67
TDS (ppm)	10	12.25	571	249.50	231.20
EC (µS/cm)	10	18.85	878	360.73	310.98

Table 5 provides overall descriptive statistics for all measured variables across both sampling rounds. The wide ranges in TDS and EC highlight spatial heterogeneity among locations, while voltage variability reflects differences in microbial electro genic activity and electrode–biofilm interactions.

Table 6. Pearson correlation coefficients

Parameter	V	pH	T (°C)	TDS	EC
Voltage (V)	1	0.21	0.18	0.09	0.11
pH	0.21	1	–0.31	–0.28	–0.27
Temperature (°C)	0.18	–0.31	1	0.06	0.05
TDS	0.09	–0.28	0.06	1	**0.998**
EC	0.11	–0.27	0.05	**0.998**	1

Table 6 presents Pearson correlation coefficients evaluating relationships between voltage output and physicochemical parameters. Voltage shows weak correlations with all environmental variables, whereas TDS and EC exhibit an extremely strong positive correlation ($r \approx 0.998$), reflecting their shared dependence on ionic concentration.

Note: TDS and EC show an extremely strong correlation ($r \approx 0.998$), consistent with known physical principles. ANOVA compares the **five locations** using the **average TDS** values from the two rounds.

Table 7. ANOVA for TDS differences between locations

Source	Sum of Squares	df	Mean Square	F	Sig.
Between Groups	56620.48	4	14155.12	25.59	**0.000**
Within Groups	2769.74	5	553.95	—	—
Total	59390.22	9	—	—	—

Table 7 summarizes the one-way ANOVA results comparing average TDS values across the five sampling locations. The statistically significant F-value ($p < 0.001$) indicates substantial spatial variation in dissolved solids, reflecting differences in ionic composition and environmental conditions among sites.

Across the five locations, TDS ranged from 12.25 to 572 ppm, with the highest values observed in the Kufa River and the lowest in Baher Al-Najaf (Figure 2). EC showed a strong positive relationship with TDS (Figure 3), varying between 18.85 and 880 µS/cm. pH values were mostly alkaline (7.4–9.9) (Figure 4). Temperature remained relatively stable across locations and days (19.6–21.9°C). Voltage measurements ranged from 0.22 to 0.60 V, with notable temporal fluctuations during daily sampling (Figure 5).

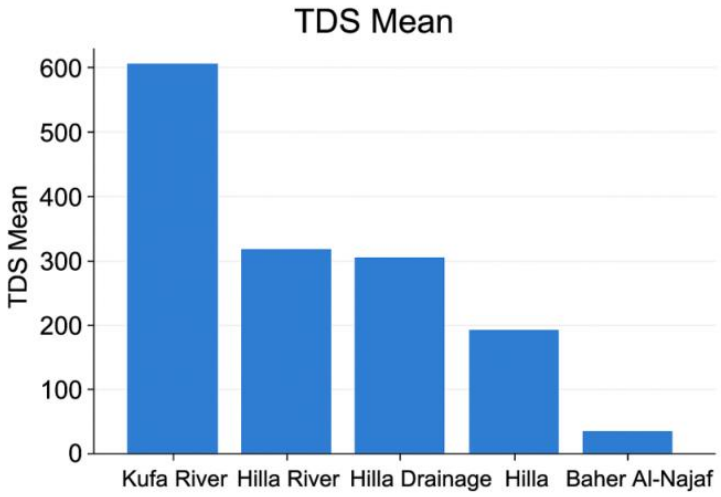

Figure 2. Spatial comparison of TDS

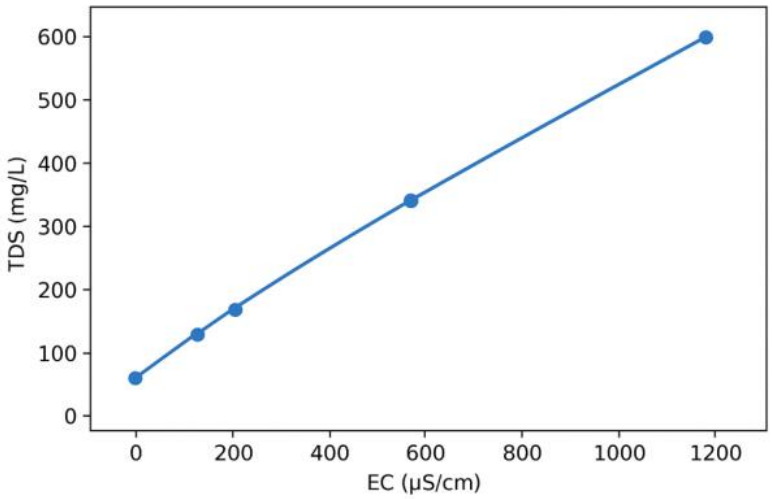

Figure 3. Scatter plot (EC vs. TDS)

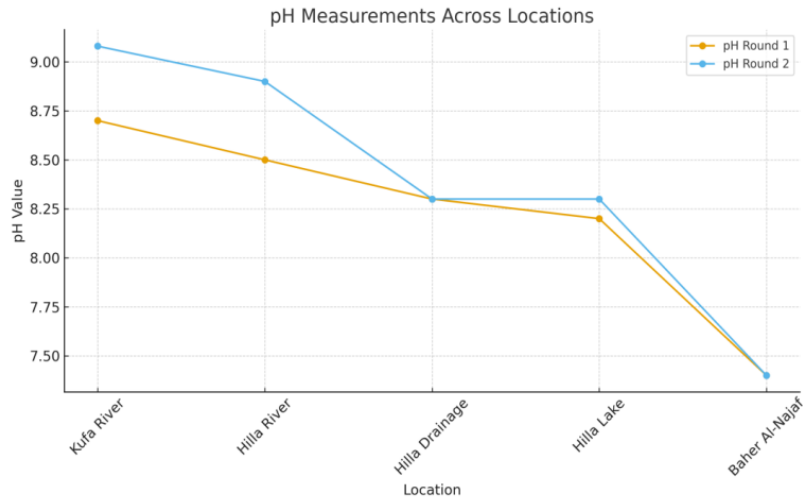

Figure 4. PH variation (round 1 vs round 2)

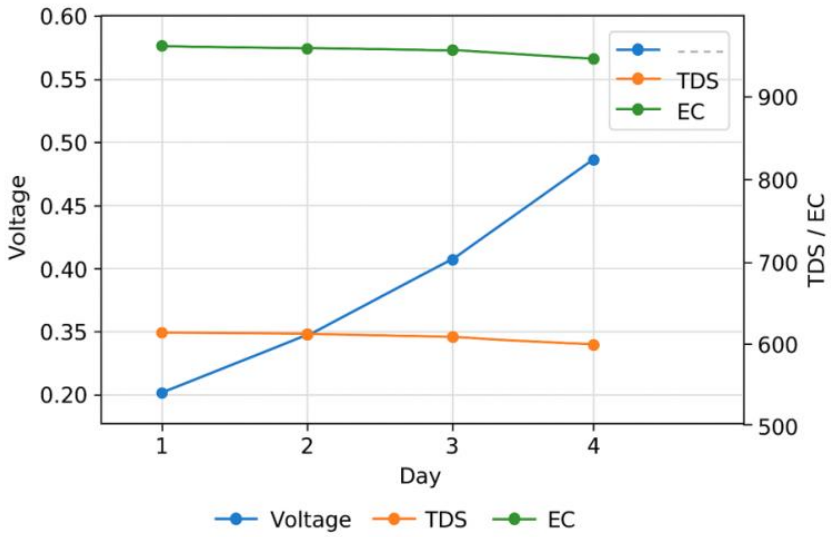

Figure 5. Four-Day time trend (V, TDS, EC)

Discussion

The results demonstrate that banana-peel waste is a viable substrate for MFC operation, while native Iraqi microbial communities exhibit strong electrogenic potential. The weak statistical dependence of voltage on physicochemical parameters suggests that electrode design and biofilm characteristics are the primary performance drivers. Nanoparticle integration is therefore expected to play a decisive role in future system optimization. The weak correlations between voltage and water physicochemical parameters (EC, TDS, pH) imply that environmental factors contribute minimally to performance. Instead, electron-transfer efficiency appears strongly dependent on: Electrode composition and surface area, Biofilm development, Presence of conductive nanoparticles, Anaerobic microbial abundance. Similar studies have shown that nanoparticles significantly improve MFC power density through catalytic activity and enhanced electron mobility. Figure 6 shows correlation of factors (pH – EC – TDS – Voltage).

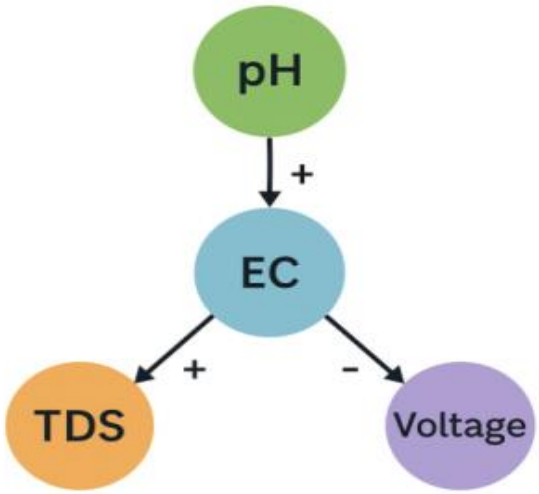

Figure 6. Schema of the correlation of factors (pH – EC – TDS – Voltage)

Nanoparticles in Microbial Fuel Cells

Nanoparticles play a transformative role in improving MFC efficiency. Their impacts include:

A. Enhanced Electron Transfer

Metal oxide nanoparticles (e.g., Fe_3O_4, TiO_2, MnO_2) promote rapid electron flow between bacterial cells and the electrode.

B. Larger Biofilm Growth

Increased surface area allows denser microbial colonization, boosting metabolic activity.

C. Reduced Charge-Transfer Resistance

Nanomaterials improve electrode conductivity and facilitate substrate oxidation.

D. Improved Cathodic Reactions

Graphene and AuNPs enhance oxygen reduction reactions at the cathode. These improvements collectively enhance power density and stability in MFC operation.

Conclusions

This study confirms the feasibility of using locally sourced waste and microbial resources for bioelectricity generation in Iraq. Voltage outputs up to 0.66 V were achieved after biofilm development. Mathematical modeling and statistical analysis revealed that microbial activity and electrode properties dominate system behavior. Future work should focus on nanoparticle-modified electrodes, advanced membranes, and system scaling for real-world applications.

Acknowledgment

The authors thank the University of Kufa for financial and logistical support. We also acknowledge the authors of the primary datasets used in synthesis.

Author Contributions

Conceptualization: Ahmed A. Abbas, Basim A. Almayahi. Data curation: Sarah A. Shakir. Methodology and formal analysis: Basim A. Almayahi. Writing—original draft: Ahmed A. Abbas, Sarah A. Shakir. Writing—review & editing: All authors have read and approved the final manuscript.

Declaration of Interests

The authors declare no competing interests.

References

Abd-Elrahman, N. K., Al-Harbi, N., Basfer, N. M., Al-Hadeethi, Y., Umar, A., & Akbar, S. (2022). Applications of nanomaterials in microbial fuel cells: a review. *Molecules*, *27*(21), 7483. https://doi.org/10.3390/molecules27217483

Aelterman, P., Rabaey, K., Clauwaert, P., & Verstraete, W. (2006). Microbial fuel cells for wastewater treatment. *Water Science and Technology*, *54*(8), 9-15. https://doi.org/10.2166/wst.2006.702

Alazmi, A., Rasul, S., & Costa, P. M. (2020). Reduced graphene oxide as a multifunctional electrode material in bioelectrochemical systems. *Journal of Power Sources, 450,* 227678.

Ammar, S. (2023). Metal oxide nanostructures for microbial fuel cell electrodes: A review. *Renewable and Sustainable Energy Reviews, 169,* 112953.

Bosco, R. M., & Aleem, F. M. (2023). Nano-encapsulated biostimulants for improving photosynthetic efficiency in capsicum under heat stress. *National Journal of Plant Sciences and Smart Horticulture, 1*(1), 9-16.

Fogel, R., & Limson, J. L. (2016). Applications of nanomaterials in microbial fuel cells. In *Nanomaterials for fuel cell catalysis* (pp. 551-575). Cham: Springer International Publishing. https://doi.org/10.1007/978-3-319-29930-3_14

Ghasemi, M., Azadfallah, M., Ismail, M., Shamsuddin, M., Jahim, J., Sedighi, M., & Wan Ab Karim Ghani, W. A. (2018). Nanostructured conductive catalysts in microbial fuel cells. *International Journal of Hydrogen Energy*, *43*(47), 21651–21667.

Gupta, A., Sharma, K., & Singhal, A. (2022). TiO_2-based nanocomposites for environmental and energy applications. *Materials Today Chemistry, 23,* 100699.

Hernández-Fernández, F. J., Pérez de los Ríos, A., Mateo-Ramírez, F., Gómez, D., Rubio, M., & Alcaraz-Monge, E. (2021). Bioelectrochemical systems for bioenergy production: Advances and challenges. *Biotechnology Advances, 49,* 107759.

Jadhav, G. S., Ghangrekar, M. M., & Chatterjee, P. (2017). Effects of electrode materials and nanomaterial modification on performance of microbial fuel cells. *Journal of Environmental Management, 201,* 243–251.

Johari, R., Sonker, R. K., Johari, R., Samariya, U., Kumar, P., Singh, P. K., & Khan, Z. H. (2025). Graphene Oxide-Based Hybrid Composite Films for Fuel Cell Applications. In *Low-Dimensional Multifunctional Hybrid Nanostructured Materials: Energy and Environmental Applications* (pp. 239-258). Singapore: Springer Nature Singapore. https://doi.org/10.1007/978-981-96-7952-2_10

Kondrotaitė-Intė, T., Zinovičius, A., Pirštelis, D., & Morkvėnaitė, I. (2025). Enhancing Electron Transfer Efficiency in Microbial Fuel Cells Through Gold Nanoparticle Modification of Saccharomyces cerevisiae. *Microorganisms, 13*(8), 1938. https://doi.org/10.3390/microorganisms13081938

Kumar, A., Siddiqui, T., Pandit, S., Roy, A., Gacem, A., Souwaileh, A. A., ... & Park, H. K. (2023). Application of biogenic TiO2 nanoparticles as ORR catalysts on cathode for enhanced performance of microbial fuel cell. *Catalysts, 13*(6), 937. https://doi.org/10.3390/catal13060937

Kumar, R., Singh, L., & Wahid, Z. A. (2015). Role of graphene-based nanomaterials in bioelectrochemical systems. *Renewable and Sustainable Energy Reviews, 45,* 546–558.

Li, C., & Sun, F. (2021). Graphene-assisted sensor for rapid detection of antibiotic resistance in Escherichia coli. *Frontiers in Chemistry, 9,* 696906. https://doi.org/10.3389/fchem.2021.696906

Liu, X., Zhao, M., & Wang, S. (2020). TiO_2 nanomaterial-based photocatalytic electrodes in bioelectrochemical systems. *Applied Catalysis B: Environmental, 278,* 119311.

Logan, B. E., & Rabaey, K. (2012). Conversion of wastes into bioelectricity and chemicals by using microbial electrochemical technologies. *science, 337*(6095), 686-690. https://doi.org/10.1126/science.1217412

Logan, B. E., Hamelers, B., Rozendal, R., Schröder, U., Keller, J., Freguia, S., ... & Rabaey, K. (2006). Microbial fuel cells: methodology and technology. *Environmental science & technology*, *40*(17), 5181-5192. https://doi.org/10.1021/es0605016

Magotra, V. K., Kang, T. W., Ahmed, A. T. A., Inamdar, A. I., Im, H., Ghodake, G., ... & Kumar, S. (2021). Effect of gold nanoparticles laced anode on the bio-electro-catalytic activity and power generation ability of compost based microbial fuel cell as a coin cell sized device. *Biomass and Bioenergy*, *152*, 106200. https://doi.org/10.1016/j.biombioe.2021.106200

Nosek, D., Mikołajczyk, T., & Cydzik-Kwiatkowska, A. (2024). Enhancing microbial fuel cell performance: anode modification with reduced graphene oxide and iron (III) for improved electricity generation. *Clean Technologies and Environmental Policy*, *26*(12), 4095-4112. https://doi.org/10.1007/s10098-024-02820-3

Osman, S. H., Kamarudin, S. K., Karim, N. A., & Basri, S. (2021). Application of graphene in low-temperature fuel cell technology: An overview. *International Journal of Energy Research*, *45*(13), 18318-18336. https://doi.org/10.1002/er.6969

Peng, L., You, S., Wang, J., & Zhang, X. (2019). Nanomaterials for enhancing the power generation of microbial fuel cells. *Advanced Functional Materials, 29*(31), 1901834.

Premalatha, M., & Abbasi, T. (2018). Graphene–TiO_2 nanocomposites for photoelectrochemical energy applications. *Journal of Industrial and Engineering Chemistry, 65,* 239–255.

Rabaey, K., & Verstraete, W. (2005). Microbial fuel cells: novel biotechnology for energy generation. *TRENDS in Biotechnology, 23*(6), 291-298. https://doi.org/10.1016/j.tibtech.2005.04.008

Rimada, Y. (2025). Sustainable Construction and Urban Water Systems: Innovations in Green Materials and Integrated Waste water Management. *Journal of Smart Infrastructure and Environmental Sustainability, 2*(3), 32-39.

Wang, J., Li, B., Wang, S., Liu, T., Jia, B., Liu, W., & Dong, P. (2022). Metal-organic framework-derived iron oxide modified carbon cloth as a high-power density microbial fuel cell anode. *Journal of Cleaner Production, 341,* 130725. https://doi.org/10.1016/j.jclepro.2022.130725

Wang, J., Zhang, P., Yang, B., Yang, S., Tong, X., Wang, M., ... & Yang, S. (2025). Cu/TiO2 nanoparticles: Enhancing microbial fuel cell performance as photocathode catalysts. *Bioresource Technology, 430,* 132586. https://doi.org/10.1016/j.biortech.2025.132586

Zhang, Y., Sun, J., Hu, Y., Hou, B., & Li, X. (2018). Enhanced bioelectricity generation by Fe_2O_3 nanoparticle-modified anodes in microbial fuel cells. *Electrochimica Acta, 259,* 415–423.